IEEE Transactions on Instrumentation and Measurement 62 (2013) 5-May, pp. 932-941

DOI:10.1109/TIM.2012.2223332

Antenna Parametrization for the Detection of Partial Discharges

Guillermo Robles, *Senior Member, IEEE*, Matilde Sánchez-Fernández, Ricardo Albarracín Sánchez, Mónica V. Rojas-Moreno, Eva Rajo-Iglesias, *Senior Member, IEEE*, and Juan Manuel Martínez-Tarifa

***Abstract*—Partial discharge (PD) detection is a widely extended technique for electrical insulation diagnosis. Ultrahigh-frequency detection techniques appear as a feasible alternative to traditional methods owing to their inherent advantages such as the capability to detect PDs online and to locate the piece of equipment with insulation problems in substations and cables. In this paper, four antennas are thoroughly studied by means of their theoretical and experimental behavior when measuring electromagnetic pulses radiated by PD activity. The theoretic study of the band of frequencies in which the pulse emits and the measurement of the parameters S_{11} are complemented with the frequency response and wavelet transform of a set of 500 time signals acquired by the antennas, and the results are analyzed in detail.**

***Index Terms*—Antenna measurements, dielectric measurements, partial discharges (PDs), UHF measurements, ultrahigh-frequency (UHF) antennas, wavelets.**

I. Introduction

ELECTRICAL INSULATION is a key issue in power system reliability. It is well known that oil-impregnated paper in power transformers, epoxy resins in generators, and polyethylene in power cables are subjected to several mechanical, thermal, and electrical stresses that degrade their behavior, leading to unexpected failures of these expensive assets and to power outages [1]. A well-known aging mechanism of electrical stress is partial discharge (PD) activity [2]. PDs are low-energy ionizations that take place in microscopic sites of electrical insulation due to its lack of homogeneity in permittivity and dielectric strength. This is typical in air voids within solid and liquid insulations where, even rated voltages applied to the power apparatus, provoke ionizations of the air. PDs do not cause an immediate failure of electrical insulation but degrade its properties due to chemical and physical attack [3]. Moreover, PDs can be a symptom of other aging mechanisms mentioned previously [4]. For all these reasons, PD measurements have been standardized as tests for electrical equipment maintenance [5]. In these classical tests, a capacitive branch is connected to the equipment terminals to detect high-frequency pulses created from PD. The pulse amplitude is represented superimposed to the phase of the applied voltage (phase resolved PD patterns) in order to distinguish between different kinds of PDs [2]. However, PD measurements are usually made in industrial facilities where high levels of electrical noise are always present. This makes difficult the interpretation of the PD pattern and the diagnosis of the insulation. PD recognition is done by analyzing PD pulse waveforms acquired with inductive devices as high-frequency current transformers (HFCTs), Rogowski coils, or inductive loops [6]–[8]. In any case, these measurements require the disconnection of electrical equipment before installing the measurement setup. In addition, all these techniques cannot locate PD sources geometrically, which could be useful for power equipment maintenance. Electroacoustic and ultrahigh-frequency (UHF) emissions from PDs can be measured to overcome these limitations [9]. The first option uses piezoelectric sensors to detect pressure waves propagating through oil, which rejects any electrical noise coupling to the acquired signals [10]. However, these sensors cannot detect PD occurring inside solid dielectrics; they have typically low sensitivity and narrow band, which makes it difficult to detect PDs that are close in time [9]. As mentioned before, another new research trend for PD detection is the use of antennas for UHF detection of PDs. This technique is based on noncontact measurements, so its application to online measurements is appropriate [11]–[13]. These sensors can also be used for any kind of insulating material and give excellent results in PD location in large facilities such as substations [14]. Moreover, the increasing number of high-voltage (HV) dc applications in power grids requires that PDs are detected without synchronization signals [15], which can be solved with antennas. The main drawback of PD detection through antennas is the presence of noise sources due to FM, television (TV), Global System for Mobile Communications (GSM), and WiFi emissions, so the antenna response to both PD and noise is an interesting research topic for PD detection [16], [17]. The comparison of several antennas had been presented before [12], but a deeper analytical background for these devices (monopole, zigzag, cone shaped, etc.) was missing in order to model PD and noise detection capability. A good theoretical model for patch antennas is found in [18] and [19], but the response to PD and noise sources is not presented.

This paper is an important step forward in the modeling of the antennas and the study of the PD power with respect to the results presented in [17], where the authors compared the power spectra for different types of antennas when measuring internal

This work was supported by the Spanish Science and Technology Ministry under Contracts DPI 2009-14628-C03-02 and TEC 2011- 29006-C03-03.

G. Robles, R. Albarracín Sánchez, M. V. Rojas-Moreno, and J. M. Martínez-Tarifa are with the Departamento de Ingeniería Eléctrica, Universidad Carlos III de Madrid, 28911 Leganés, Spain (e-mail: grobles@ing.uc3m.es).

M. Sánchez-Fernández and E. Rajo-Iglesias are with the Departamento de Teoría de la Señal y Comunicaciones, Universidad Carlos III de Madrid, 28911 Leganés, Spain.

PDs without any further analysis on the antenna design and parametrization. First, through a typical Gaussian pulse model for PD, the spectrum of the signal derived in the antenna is analytically obtained. Furthermore, a relationship between the half-amplitude PD pulsewidth and the PD placing in frequency and its bandwidth is given. Second, S_{11} parameters are measured to validate the antenna design and the antenna matching, to ensure that the manufacturing has been correct, and to guarantee that the antennas will measure in the band of frequencies of interest. Additionally, the S_{11} is measured for antennas with and without ground plane. Third, a new test object is designed to create a cylindrical hollow inside a stack of transformer paper layers and to control the PD activity and the results derived from their study. Fourth, new energy studies are done based on the wavelet transform and representing the energy in different bands of frequency to compare the behavior of the antennas.

In summary, in this paper, four different types of antennas, i.e., two monopoles with different lengths, a trapezoidal zigzag antenna, and a commercial logperiodic antenna, are studied as candidates to measure PDs. In Section II, PD electromagnetic emission is characterized in order to find the target band of frequencies where the manufactured antennas should work; also, the design and important parameters of the antennas are shown, and the S_{11} parameter is measured for all of them. Section III explains the measuring setup to generate and detect PDs. Finally, Section IV shows the measurements and the study in the frequency domain of the pulses acquired with the antennas to conclude that theoretical and experimental results match and, specifically, monopole antennas are good candidates as sensors for PD detection.

II. Modeling of the Antennas

When designing an antenna for sensing purposes, one of the key issues to take into account is the type of signal that this antenna should detect, specifically the bandwidth that the signal occupies. A simplified model for the PD pulses can be found in the literature [18], where the waveform is modeled with a Gaussian shape and the half-amplitude width is given by a parameter T_h. The response of the antenna follows the time derivative of the PD current $I(t)$, and therefore, under this model, the spectrum $\mathcal{S}_{\mathrm{PD}}(f)$ of the signal that the antenna should detect can be easily obtained. If the normalized $(I_0 = 1)$ PD waveform is given by

$$I(t) = I_0 e^{-\left(\frac{t}{t_0}\right)^2} \tag{1}$$

where $t_0 = T_h/2\sqrt{\log 2}$, then the amplitude of the spectrum sensed would have the form

$$|\mathcal{S}_{\mathrm{PD}}(f)| = 2\pi\sqrt{\pi} f t_0 e^{-\frac{(2\pi f t_0)^2}{4}} \tag{2}$$

also plotted in Fig. 1.

It should be noticed that, through that formulation, the spectrum has been characterized in terms of the normalized frequency $f_n = f \times T_h$. This allows, by solving numerically for the 3-dB bandwidth, to obtain the PD bandwidth in terms

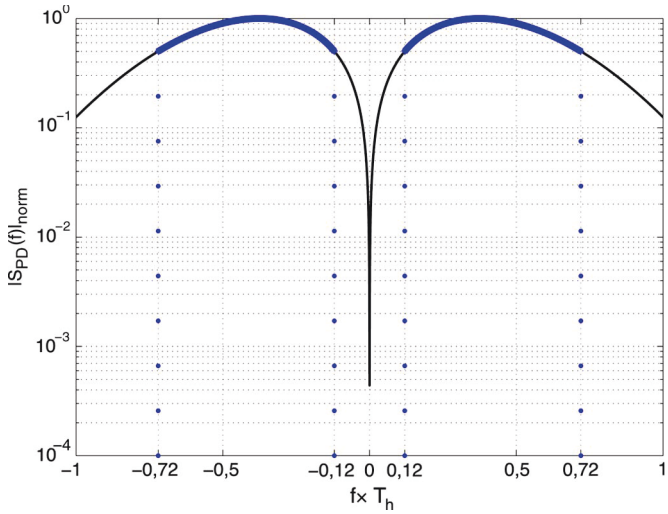

Fig. 1. Approximate bandwidth of the detected PD generated signal.

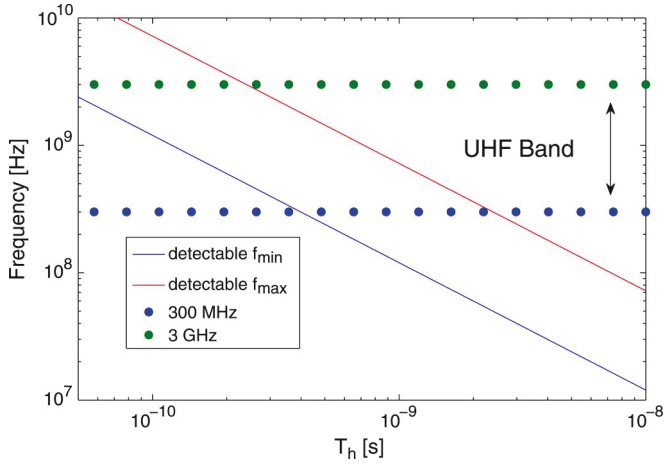

Fig. 2. Range of T_h values that fall within the UHF band.

of the T_h parameter. For that, it is necessary to obtain the two solutions $f_n^{\min}$ and $f_n^{\max}$ for $f_n \geq 0$ from this equation

$$\frac{1}{2}\max_{f_n}|\mathcal{S}_{\mathrm{PD}}(f_n)| = \frac{\pi\sqrt{\pi}}{\sqrt{\log 2}} f_n e^{-\frac{\pi^2 f_n^2}{4\log 2}}. \tag{3}$$

The solutions are $f_n^{\min} = 0.12$ and $f_n^{\max} = 0.72$. Consequently, the signal would be approximately located in the band of $0.12/T_h$–$0.72/T_h$ Hz, as shown marked with a thicker trace in Fig. 1. The relationship obtained given those values for the 3-dB bandwidth and considering that the typical values of T_h for internal discharges are below 1 ns will locate the detected signal in the UHF band. Those are shown in Fig. 2, where the PD bandwidth is plotted versus the T_h parameter and, as a reference, the UHF band is also given. Thus, all the antennas proposed should at least cover part of this band.

Once the antenna working frequencies are located, there are some other antenna characteristics that should be defined to specifically match our sensing environment, and those are the radiation pattern, which also characterizes the antenna directivity, and the antenna efficiency by means of the S_{11} parameter.

The radiation pattern needed is determinant in the design of an antenna, and our focus for the application addressed should be radiation patterns with medium to low directivity,

for instance, omnidirectional ones. The reason for that is that, although, in our case study, the measurement environment is controlled and, therefore, we have information about the position of the PD source, it is still interesting to cover as many directions for incoming power as possible, showing this way the suitability of the proposed designs where the source of PD is not clearly located. Also, simple designs are of interest, since, once we had shown the validity of the proposed antennas in the testing scenario, large deployment of elements is typically needed for monitoring and location leveraging the importance of inexpensive sensors.

The antenna efficiency is the second parameter to be taken into account when designing antennas. Efficiency depends on the antenna losses given by the ohmic losses of materials (metals and dielectric) and also on the mismatching losses, i.e., the S_{11} parameter. In simple resonant antennas and in the low-frequency range, we are targeting, the ohmic losses are negligible, and the antenna efficiency can be defined as $e = 1 - |S_{11}|^2$. Thus, the S_{11} parameter would be the reference measurement to determine the resonant frequency of the antenna, the range of frequencies where the antenna is well matched (antenna bandwidth),[1] and also the key parameter to determine the antenna efficiency for each of the working frequencies of the antenna.

Monopole antennas hold the design needs mentioned so far: They are simple and have omnidirectional patterns, and in addition to that, it is relatively simple to tune the antenna to work in a particular range of frequencies [13]. The monopole antenna in its basic design consists of a wire with a length of approximately $\lambda/4$, with λ being the wavelength of the main frequency tuned [20]. Compared to a dipole, this antenna does not need a balun, and this makes it much more convenient and, therefore, more used in practice. In theory, this antenna should have an "infinite" ground plane to have a good behavior and also to achieve the omnidirectional radiation pattern with a maximum directivity of around 5 dB.

Thus, the radiation pattern of an ideal $\lambda/4$ monopole antenna has a shape as

$$r(\theta, \phi) = \frac{\cos^2\left(\frac{\pi}{2}\cos(\theta)\right)}{\sin^2(\theta)} \tag{4}$$

where ϕ $(0 \leq \phi \leq 2\pi)$ is the azimuth angle defined in the $(\hat{x}\hat{y})$ plane, θ $(0 \leq \theta \leq \pi/2)$ is the elevation angle, and we assume that the monopole antenna has its axis along the $\hat{z}$-direction, as it is shown in Fig. 3. It should be noted that the radiation pattern does not depend on ϕ, leading to the omniazimuthal (radiation all around the wire with rotational symmetry) radiation pattern, and also that, given the infinite ground plane, it radiates only in half-space.

When the monopole has a truncated ground plane of not many wavelengths, the directivity is reduced. We must remember here that the directivity gives the limit value for the antenna gain, which is the product of directivity and efficiency. Nevertheless, it should also be said that it is always possible to

[1]The reference value to consider that the antenna is well matched is typically below -10 dB.

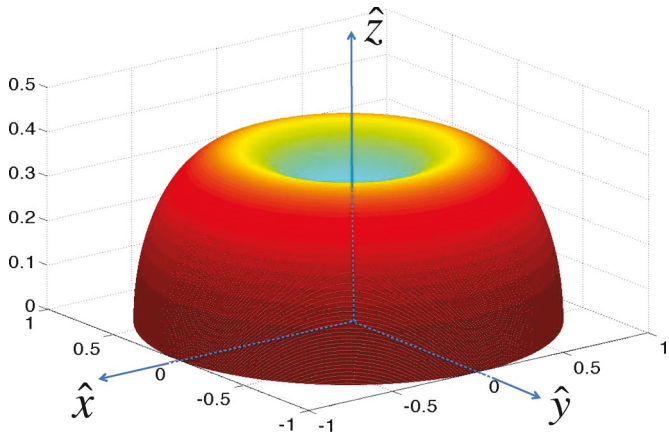

Fig. 3. Theoretical normalized radiation pattern for a $\lambda/4$ monopole.

do a monopole antenna without ground plane. In this case, all surrounding objects act as ground plane, and we can see how the antenna still works. However, the efficiency is reduced, and sometimes, the operating frequency is shifted with respect to the theoretical one. Also, different manufacturing methods of monopole antennas could lead to slights variations with respect to the ideal radiation pattern, but in general terms, all of them keep the zero radiation in the direction of the axis $\hat{z}$ and a similar level of radiation in all the azimuthal directions.

We suggest then to use three different monopoles that have been manufactured with this aim with and without ground plane. Two of them will have different lengths to cover the target range of frequencies, and for the last one, a zigzag geometry is proposed, which is known to help as well in matching and, therefore, could be more efficient. The first monopole design is 5 cm in length. With that, the theoretical resonant frequency is at 1.5 GHz, and its directivities are around 2 dB for the deployment without ground plane and 5 dB for the infinite ground plane. The second monopole is 10 cm in length, and this again leads to a 750-MHz resonating frequency and the same directivities as those for the 5-cm case. The zigzag geometry antenna has a maximum length of 10 cm (16.5 cm when it is straightened), and therefore, its behavior is supposed to be in between the one of the 10-cm monopole and that corresponding to a monopole with 16.5 cm (which has a 450-MHz resonance frequency). The zigzag geometry can have advantages in terms of efficiency (matching) when the antenna has no ground plane.

A fourth antenna is also proposed to be used in the testing environment, and this is a commercial logperiodic antenna UHALP 91088A [21], which is a wideband antenna. This antenna is physically much bigger than the previous proposed dipoles (the largest dimension is 54 cm) and, therefore, does not match our requirement for simple designs. However, it is also interesting to measure with this antenna for comparison purposes and with the idea of scanning a large number of frequencies for PD detection. In the working band of the antenna, its gain is around 6–7 dB according to the manufacturer. Another important consideration is that the antenna has a "pencil-type" radiation pattern pointing in the direction of its axis.

In order to validate the proposed antenna designs and to determine the real matching frequencies, the S_{11} parameter has been measured for the manufactured antennas and also

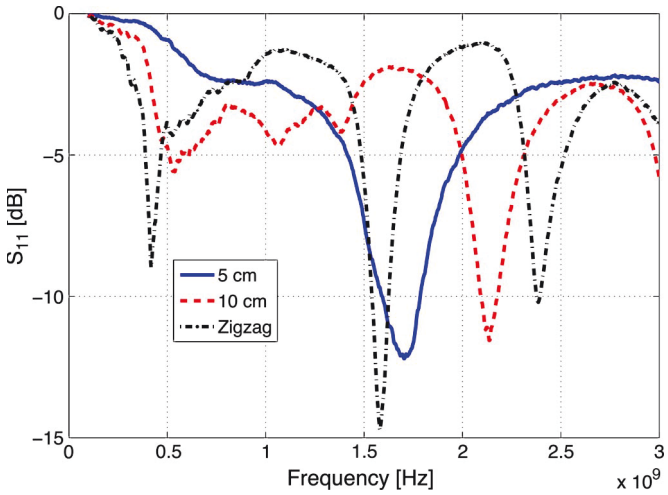

Fig. 4. Measured S_{11} parameter for the manufactured antennas without ground plane.

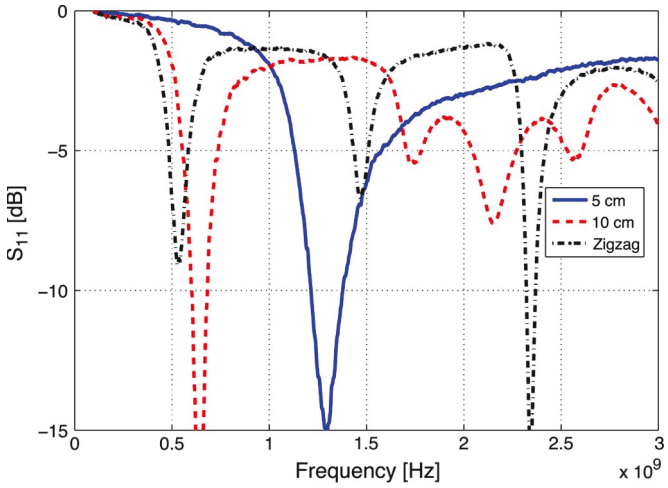

Fig. 5. Measured S_{11} parameter for the manufactured antennas with ground plane.

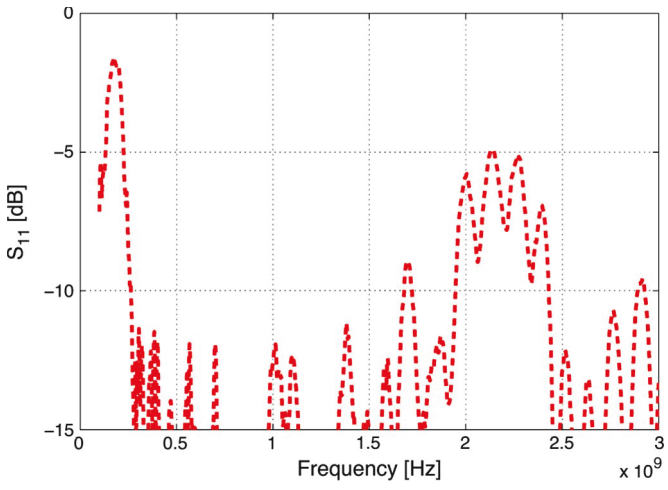

Fig. 6. Measured S_{11} parameter for the commercial antenna.

for the commercial one with an Agilent Technologies E8364B (10 MHz–50 GHz) programmable network analyzer in a laboratory facility (unshielded environment). The results are shown in Figs. 4–6.

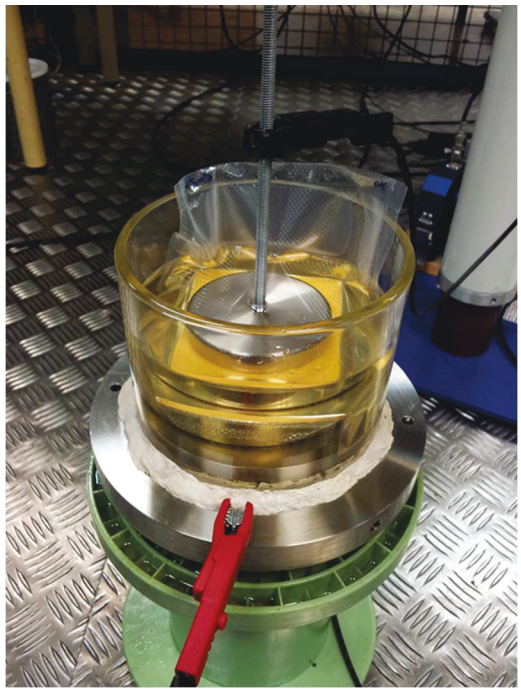

Fig. 7. Test object particularly designed to have internal discharges inside a cylindric void which is 1 mm in diameter and 1.75 mm in height.

If we observe the resonant frequencies and compare them with the theoretical frequencies given previously in this same section, we can detect a slight deviation in some of the values that is mainly due to the antenna manufacturing process. In any case, these deviations do not reduce the validity of the study, given that the working frequencies of the manufactured antennas are still within the target range of frequencies. Moreover, comparing Figs. 4 and 5, we can observe the benefit in terms of better adaptation of the antennas with ground plane. It should be noted that the manufactured antennas also work in harmonic frequencies as all type of resonant antennas.

III. Experimental Setup

Due to the fact that PDs are stochastic processes depending on several factors such as applied voltage level, insulation aging status, and environmental conditions [3], the setup has to be carefully designed to obtain repetitive results. Moreover, receptivity in the UHF band depends on the metallic structures around the antennas and, as tests were carried out in an HV laboratory, there were plenty of them, so the antennas had to be deployed close to the test object.

A. Test Object Design

PDs were generated in a controlled test object to ensure a constant and predictable PD activity (Fig. 7). Eleven sheets of transformer paper were cut into 8 cm × 8 cm squares and stacked, placing three sheets on top, piercing five with a needle, and placing the remaining three sheets at the bottom. The stack was introduced in a plastic bag, the air was removed with a vacuum machine, and, then, the stack was sealed. This layout creates a cylindric hole measuring 1 mm in diameter and 1.75 mm in height, where the dielectric permittivity is lower

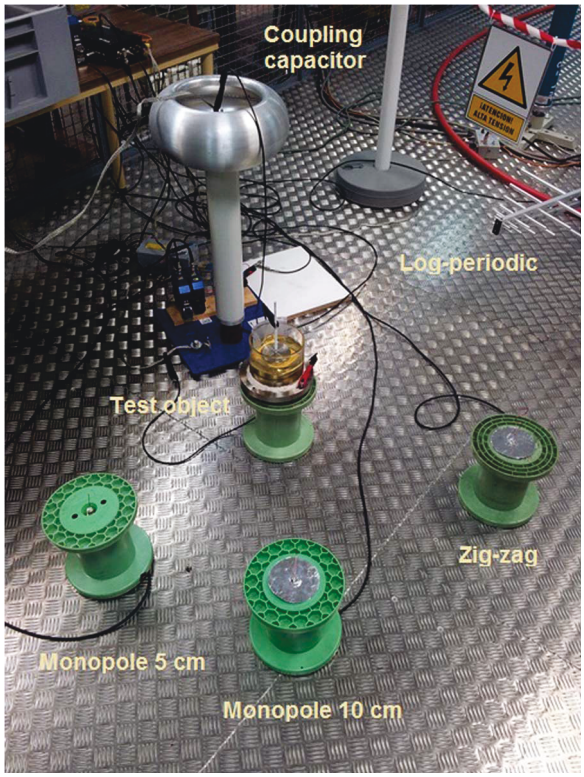

Fig. 8. Setup displaying the layout of the four antennas, the test object, and the coupling capacitor in parallel with the test object.

than the paper's. Then, the sealed stack is placed between two electrodes and immersed in transformer oil to minimize the appearance of surface discharges along the plastic bag. One of the electrodes is connected to HV, and the other is connected to ground. When HV is applied to the stack, the electric field will be larger inside the cylinder than in the rest of the homogeneous dielectric, and most of internal PDs will occur in that region.

According to standard IEC 60270, a coupling capacitor is connected in parallel to the test object to provide a path to ground for the high-frequency current pulses created by PDs (see Fig. 8). These conducted pulses are measured with an HFCT with a bandwidth up to 40 MHz connected to an oscilloscope to confirm that the detected UHF pulses are a consequence of PD activity.

The HV source is a Schleich BV 702210 transformer with a GLP1-e HV control module that can reach up to 18 kV. It has been found that PD activity starts around 10 kV and it is stable. Hence, the HV source is slowly set slightly above the inception voltage, and the measuring campaign starts. Pulses were acquired at 11 kV.

B. Antenna Deployment

As explained previously, different antennas with different frequency ranges were used to measure the radiation of PDs: a logperiodic antenna UHALP 91088A with a range from 250 MHz to 2.4 GHz, two monopole antennas which are 5 and 10 cm long, and a trapezoidal zigzag antenna. As shown in Section II, monopolar antennas with an appropriate ground plane improve the reception due to the better matching of the

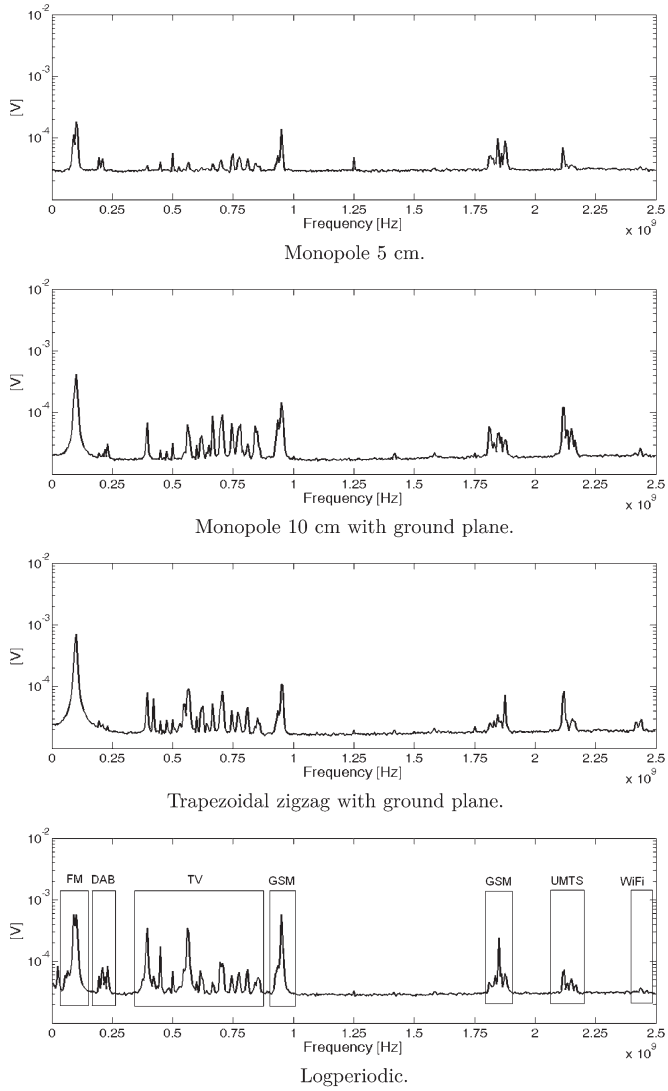

Fig. 9. Background noise spectra in volts for all the antennas.

resonant frequency and the augmented directivity. Under this assumption, two monopoles 10 cm long were manufactured, one with ground plane and the other without ground plane to measure the differences when detecting PDs. The trapezoidal zigzag antenna also had ground plane, but the monopole 5 cm long has no ground plane because it is so short that the connector behaves as ground plane.

The antennas are deployed around the test object, and their outputs are connected to an oscilloscope with RG-223 coaxial cables. The position of the antennas in the measurement environment is an important issue that should be taken into account, since the distance between the antenna and the source of the PD should force the antennas to work in the far-field region. The reason for that is to assure that we are working in a distance where the radiation pattern does not change with distance. Since the three manufactured antennas have dimensions smaller than $\lambda/2$, it is convenient that they are placed at a distance of approximately 1–2 λ (40–80 cm for the monopole 10 cm long). In the case of the logperiodic antenna, this distance must be longer as the antenna size is larger. At the same time, it should be noted that the radiated field decays inversely proportional

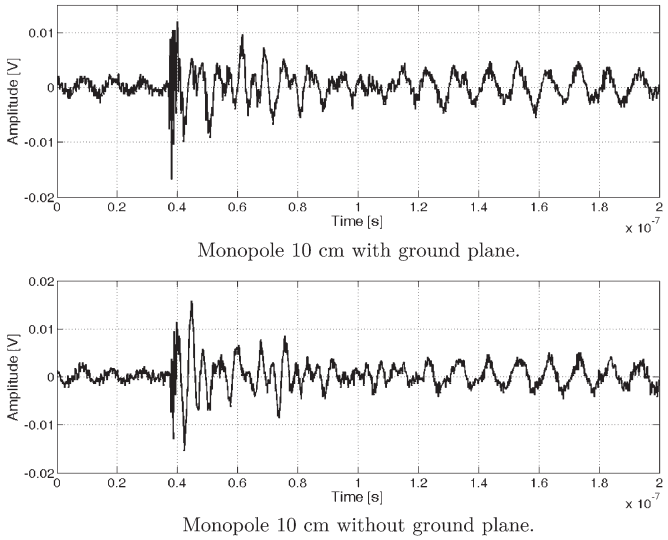

Fig. 10. PD pulses measured with two monopoles 10 cm long with and without ground plane.

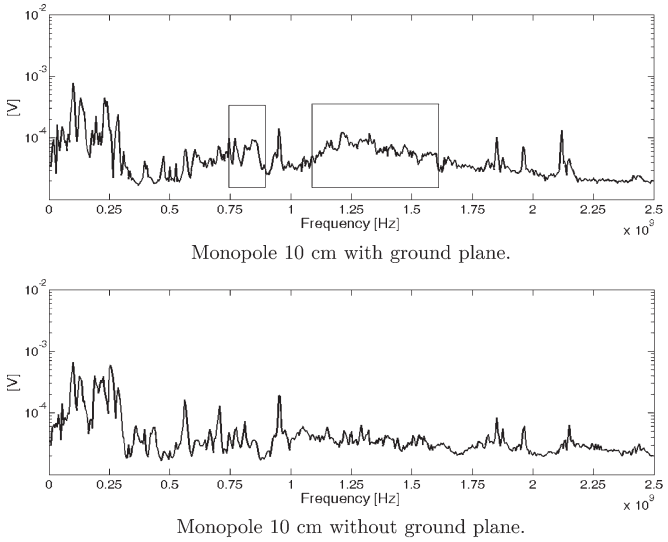

Fig. 11. PD spectra for two monopoles 10 cm long with and without ground plane.

with the distance, and when comparing received signal levels, therefore, all antennas should be placed at the same distance from the PD source. Thus, special attention has been put to maintain the same distance, 45 cm, between the test object and all the monopole antennas, showing another advantage of the use of monopolar type of antennas as we can be quite close to the source of the discharges if required. The logperiodic antenna has been placed at a longer distance, 90 cm, to ensure that it measures far-field radiation and with the dipoles parallel to ground.

UHF acquisitions were made in a Tektronix DPO7254 8-b 40-GS/s four-channel oscilloscope, where the response of each antenna to PD pulses was registered. During the experiments in the laboratory, most factors were controlled to assure uniformity in the measurements, and series of 500 pulses were recorded at 10 GS/s and processed to guarantee that the results were statistically reliable.

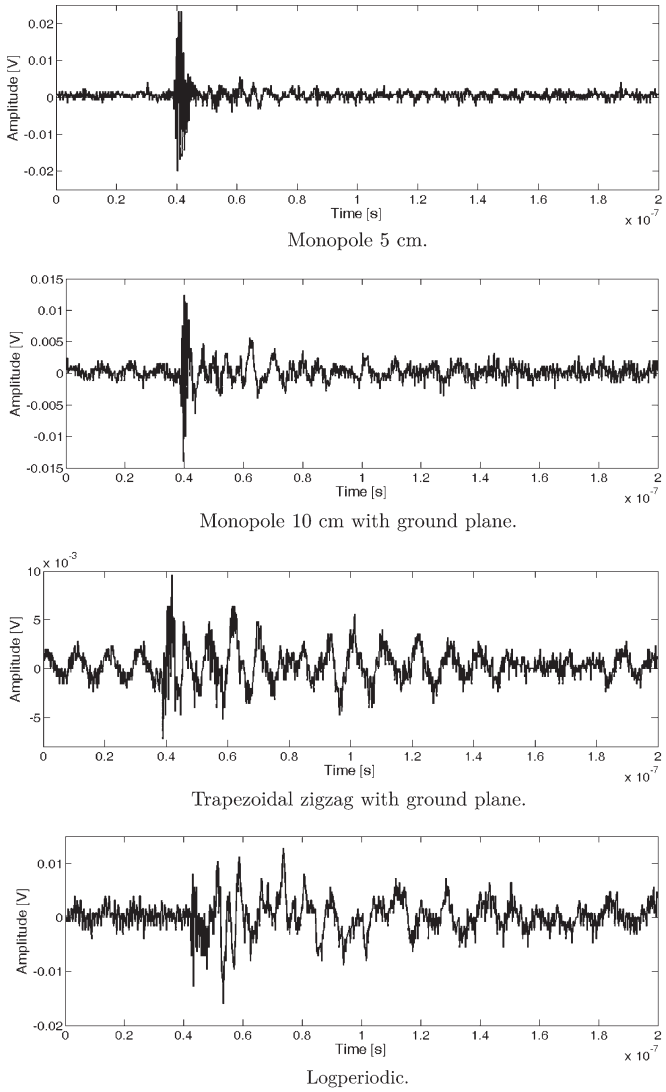

Fig. 12. PD pulse measured with every antenna.

IV. Measurements

Measurements were taken to demonstrate experimentally the theoretical results for the characterized antennas obtained in Section II. A total of 500 signals was acquired for every antenna, first without and then with PDs. The fast Fourier transform with a rectangular window was calculated for all signals to obtain the spectra and then averaged to reduce its variance. This process is repeated whenever a frequency plot is displayed in this paper.

A. Background Noise

The first step is the characterization of the background noise present in the laboratory. This is done by measuring randomly 500 time signals acquired with all of the antennas and calculating their averaged spectra. The results are shown in Fig. 9, where FM radio, digital audio broadcasting (DAB), TV broadcasting, GSM–general packet radio service, and WiFi signals are clearly captured. In some cases, the antenna behavior is already seen in this figure. The 10-cm monopole and

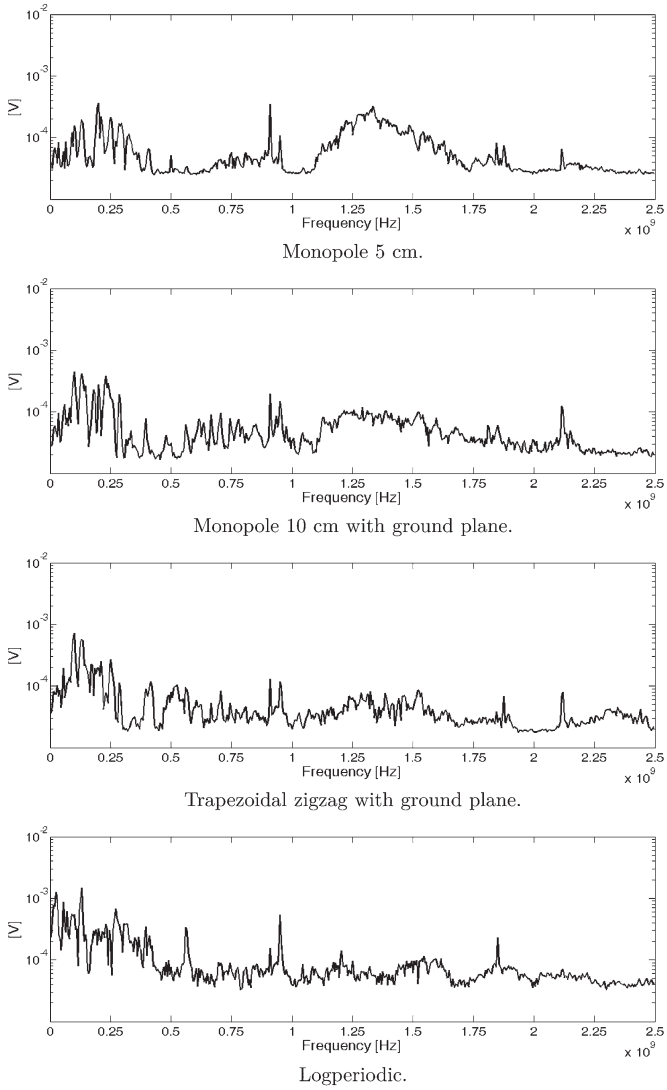

Fig. 13. Averaged spectra of 500 pulses acquired with the antennas.

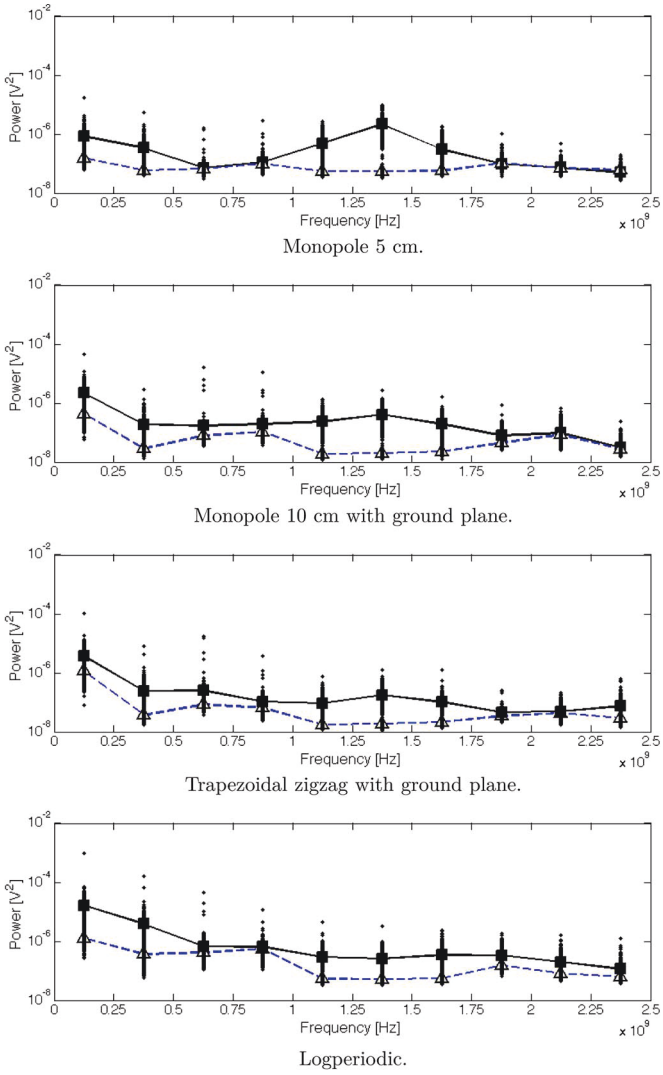

Fig. 14. Cumulative power in 250-MHz bands for 500 pulses acquired with the antennas (■) with PD and (△) without PD.

the trapezoidal zigzag antenna have good response in the TV broadcasting band, whereas the 5-cm-long monopole has a poor reception at these frequencies. The logarithmic antenna has a flat response in the range of frequencies shown in the plots according to its datasheet, so it will be used as the reference for the rest of the antennas. The background noise for the 10-cm-long monopole and the trapezoidal zigzag antenna without ground plane was also acquired and was essentially the same as that detected with the monopole with ground plane, so they have not been plotted.

B. Monopoles 10 cm Long With and Without Ground Plane

Measurements were taken with these two antennas to check if there are significant differences in the acquisitions. In the case of the monopoles 10 cm long, the main frequency is 750 MHz, so receptivity should be good at this frequency and its multiples. Fig. 10 shows two PD pulses measured with these monopoles in a time window of 200 ns at 11 kV. Although they seem to be very similar, a closer study of the front wave shows that there is a larger high-frequency content in the signal acquired with the monopole with ground plane. This is better seen in the averaged spectra of 500 pulses taken with both antennas and shown in Fig. 11. As expected, the magnitudes in the band around 750–800 MHz have been increased, demonstrating that a ground plane improves the reception. Moreover, the band from 1100 to 1600 MHz has increased noticeably with the ground plane, and it is there, precisely, where the first multiple 1500 MHz lies.

C. Antenna Behavior

The next set of measurements is done for all the antennas. Actual pulses inside the dielectric have rise times shorter than 1 ns, so according to Fig. 2, the emission will approximately be in a wide band from 100 MHz to 2 GHz. An example of a PD pulse measured with the antennas is shown in Fig. 12. The pulse starts at the same time for all of the antennas but the logperiodic antenna because it was placed farther. Although the signals are different, they have the same structure: Before the trigger, there is background noise, then there are fast variations of the signal for the first nanoseconds due to the direct

TABLE I
AVERAGE CUMULATIVE POWER IN $V^2 \times 10^{-9}$ FOR THE FOUR TYPES OF ANTENNAS MEASURING PDS AND BACKGROUND NOISE. THE COLUMNS ARE THE FREQUENCY BANDS IN MEGAHERTZ

	0-250	250-500	500-750	750-1000	1000-1250	1250-1500	1500-1750	1750-2000	2000-2250	2250-2500
5 cm	845	346	72.4	114	491	2210	306	99.1	72.6	49.5
Noise	153	59.3	67.2	98	55.6	54.5	56.9	104	70.8	60.9
10 cm	2180	186	170	195	234	399	191	78	95.7	31.6
Noise	422	28.3	77.8	106	18.7	19.9	22.5	44.4	84.2	27.2
Zigzag	3640	244	250	106	92.2	175	103	45.8	48.4	74
Noise	1140	37	84.9	64.5	17.6	18.5	21	33.9	43.1	28.9
Logperiodic	16500	3930	674	653	295	260	341	329	197	116
Noise	1260	370	409	545	53.5	52.6	55	153	81.6	63.8

wave propagation of the pulse and multipath propagation, and then there is radiation at lower frequencies due to the impulsive nature of the PD. Again, 500 time signals were acquired, and their spectra were calculated and averaged to obtain the frequency response of the antennas. The results are shown in Fig. 13. The differences with the plots in Fig. 9 are evident since there is energy in all the measured band up to 2.5 GHz that even hides strong broadcasting emissions of radio and TV. As expected, the monopole 5 cm long has an outstanding behavior in the band from 1100 to 1700 MHz and shows that PDs emit, at least, in that band. The monopole 10 cm long with ground plane has also good reception in this band but also at lower frequencies centered in 700 MHz where the 5-cm monopole is not so good. The trapezoidal zigzag antenna with ground plane has more sensitivity around 500 MHz, although it can also measure energy in the higher frequency band as the first two antennas. Finally, the logperiodic antenna captures energy in all the band as expected.

The cumulative power in bands of 250 MHz has been calculated and is plotted in Fig. 14 to have a better understanding of the power distribution in frequency. In this case, the magnitude at every frequency of the spectra is divided into $\sqrt{2}$ to obtain the root mean square and then squared to calculate the power. The powers are summed in bands of 250 MHz, and the result is the cumulative power in that band.

The cumulative power of the background noise in Fig. 9 is shown in Fig. 14 as triangles joined by a dashed line. The averaged cumulative power of the signals with PDs is presented as squares joined by a solid line. Finally, every cumulative magnitude is shown as a dot per spectrum to have a measure of the dispersion of the acquisitions.

The logperiodic antenna can be considered as the reference because it has almost a flat response up to 2.5 GHz. Then, it can be clearly seen in its frequency response that PD pulses have energy in all bands up to 1750 MHz. From this frequency, the differences between noise and PD power are negligible in all the antennas. The plot for the logperiodic antenna also shows that the increments in power compared to the background noise are quite constant in the rest of the bands. Considering this premise, the specific antenna behavior in frequency can be easily deduced from the rest of the plots. In those bands where the increment in power is larger, the antenna has better response than when the increment is lower. Then, the 5-cm monopole has an outstanding response in the band from 1250 to 1500 MHz, a good response from 1000 to 1250 MHz and from 1500 to 1750 MHz, and a very poor response in the band from 500 to 1000 MHz. The 10-cm monopole with ground plane has an overall good response from 1000 to 1750 MHz, and for the rest of the band, it is very similar to the zigzag antenna. Compared to the rest of the monopoles, the behavior of the trapezoidal zigzag antenna with ground plane is not so good in the UHF band, and it seems to be only remarkable in the lowest frequency bands from 0 to 500 MHz, although this is clarified in Table I.

TABLE II
SEVEN DETAIL LEVELS AND APPROXIMATION OF THE WAVELET DECOMPOSITION AND THEIR FREQUENCY INTERVALS IF $f_s = 10$ GHz. THE THIRD COLUMN RELATES THE BANDS WITH THE CORRESPONDING ENVIRONMENTAL NOISE

Detail	Interval (MHz)	Noise
D1	2500 - 5000	—
D2	1250 - 2500	GSM, UMTS, WiFi
D3	625 - 1250	TV, GSM
D4	312.5 - 625	TV
D5	156.25 - 312.5	DAB
D6	78.125 - 156.25	FM
D7	39.0625 - 78.125	Inductive
A1	0 - 39.0625	Inductive

This table gives the same information as Fig. 14 but specifies the numerical values. The light gray shaded cells correspond to the last columns where the differences between noise and PDs are negligible. The dark gray shaded cells are frequencies where the differences are remarkable (10 dB or more), whereas the medium gray shade represents changes of at least 7 dB. In the case of the trapezoidal zigzag antenna, the effect of the PDs is not so noticeable, and two cells have been shaded with medium gray: One of them is at low frequencies, and the other is from 1250 to 1500 MHz.

This study shows that the zigzag antenna is not a good candidate to measure PDs and, therefore, monopoles with long lengths should be discarded. However, the choice between the other two monopoles remains unclear because they seem to have similar behavior in frequency. An additional study based on the wavelet transform has been made to find out the best option. The wavelet transform decomposes the time signals into N levels of details D_n and an approximation A_1 using a filter bank. Then, the details are calculated by filtering the original signal in frequency intervals from $f_s/2^{n+1}$ to $f_s/2^n$, where f_s is the sampling frequency and n is the number of the detail. The discrete wavelet transform was done using a Daubechies wavelet with order 5 and seven levels of decomposition to cover the most important frequency intervals. These are shown for every detail in Table II. The approximation level is the signal that remains in the lower frequency interval of 0–39.0625 MHz.

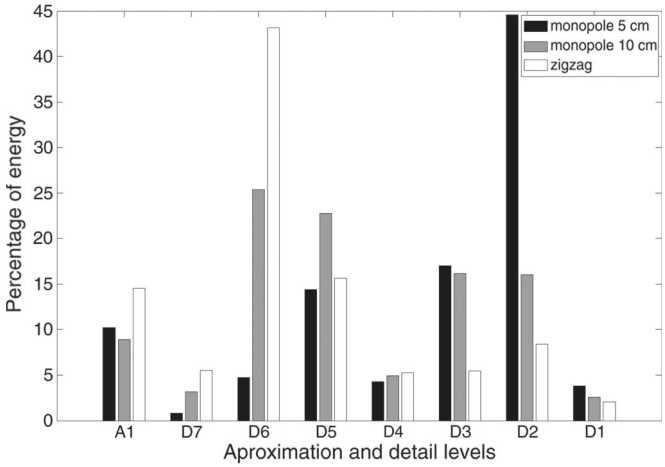

Fig. 15. Percentage of the averaged energy in the details and approximation of the discrete wavelet transform when measuring PDs.

The discrete wavelet decomposition was applied to all 500 signals from the monopole antennas when measuring PD, then the energy of the signals in the details and the approximation was calculated, and, finally, the average energy per detail and approximation was calculated. This is shown in Fig. 15 for the three monopoles. The horizontal axis of the plot contains the approximation and the details ordered in the bands of frequency in Table II, and the vertical axis represents the average energy percentage. The zigzag antenna, white bars, captures more than 40% of the energy in the band of detail 6 which is where FM radio is. The energy in detail 5, mostly corresponding to DAB radio, and the approximation, HF band, is also significative. Therefore, the zigzag antenna is working in bands where the environmental noise is important and which hide the PD pulse. In the case of the monopole 10 cm in length, more than 50% of the energy is in the very high frequency band, whereas the monopole 5 cm in length captures more than 60% of the energy in the UHF band. This energy share is expected from the results obtained for the parameter S_{11} and allows us to conclude that the shorter tested monopole is the most adequate to measure PD.

V. Conclusion

The theoretical analysis of the electromagnetic radiation of PD pulses done shows that sensors in the UHF range can detect them. Under this assumption, four antennas with different frequency behavior have been chosen to measure PDs. A deep experimental study concludes that the two monopoles 5 and 10 cm long have good responses at frequencies above 1000 MHz which corresponds to their $\lambda/4$ condition. The zigzag antenna is not so sensitive as the monopoles, but it is more appropriate for measuring at lower frequencies (below 500 MHz) because its behavior is that of a monopole with 16.5 cm in length. The logperiodic antenna is a good reference to compare the results, although its response is not so good as the monopoles for frequencies above 750 MHz. An additional study based on the wavelet transform corroborates these results and shows that the monopole 5 cm in length receives more than 60% of the energy of the radiated signal in the UHF band, designating it as the best option to measure PDs. Therefore, this phenomenon can be measured with simple and inexpensive monopoles in an efficient manner.

Acknowledgment

Tests were done in the High Voltage Research and Test Laboratory of Universidad Carlos III de Madrid.

References

[1] P. Gill, *Electrical Power Equipment Maintenance and Testing*. New York: Marcel Dekker, 1998.

[2] F. H. Kreuger, *Partial Discharge Detection in High-Voltage Equipment*. London, U.K.: Butterworths, 1989.

[3] P. Morshuis, "Degradation of solid dielectrics due to internal partial discharge: Some thoughts on progress made and where to go now," *IEEE Trans. Dielectr. Electr. Insul.*, vol. 12, no. 5, pp. 905–913, Oct. 2005.

[4] G. Stone, E. Boutler, I. Culbert, and H. Dhirani, *Electrical Insulation for Rotating Machines: Design, Evaluation, Ageing, Testing and Repair*. Piscataway, NJ: IEEE Press, 2004, ser. Series on Power Engineering.

[5] *High Voltage Test Techniques. Partial Discharge Measurements*, IEC 60270, 2000.

[6] G. Robles, J. M. Martínez, M. Rojas, and J. Sanz, "Inductive sensor for measuring high frequency partial discharges within electrical insulation," *IEEE Trans. Instrum. Meas.*, vol. 58, no. 11, pp. 3907–3913, Nov. 2009.

[7] D. Ward and J. Exon, "Using Rogowski coils for transient current measurements," *Eng. Sci. Educ. J.*, vol. 2, no. 3, pp. 105–103, Jun. 1993.

[8] M. Argüeso, G. Robles, and J. Sanz, "Implementation of a Rogowski coil for the measurement of partial discharges," *Rev. Sci. Instrum.*, vol. 76, no. 6, p. 065107, Jun. 2005.

[9] S. M. Markalous, S. Tenbohlen, and K. Feser, "Detection and location of partial discharges in power transformers using acoustic and electromagnetic signals," *IEEE Trans. Dielectr. Electr. Insul.*, vol. 15, no. 6, pp. 1576–1583, Dec. 2008.

[10] J. Ramírez-Niño and A. Pascacio, "Acoustic measuring of partial discharge in power transformers," *Meas. Sci. Technol.*, vol. 20, no. 11, p. 115 108, Nov. 2009.

[11] S. Tenbohlen, D. Denissov, S. Hoek, and S. Markalous, "Partial discharge measurement in the ultra high frequency (UHF) range," *IEEE Trans. Dielectr. Electr. Insul.*, vol. 15, no. 6, pp. 1544–1552, Dec. 2008.

[12] J. López-Roldán, T. Tang, and M. Gaskin, "Optimisation of a sensor for onsite detection of partial discharges in power transformers by the UHF method," *IEEE Trans. Dielectr. Electr. Insul.*, vol. 15, no. 6, pp. 1634–1639, Dec. 2008.

[13] C.-H. Jin, J.-Y. Lee, D.-W. Park, and G.-S. Kil, "Detection of partial discharges by a monopole antenna in insulation oil," in *Proc. 11th/12th WSEAS Int. Conf. IMMURO*, Stevens Point, Wisconsin, 2012, pp. 27–30.

[14] I. Portugués, P. Moore, I. Glover, C. Johnstone, R. McKosky, M. Goff, and L. van der Zel, "RF-Based partial discharge early warning system for air-insulated substations," *IEEE Trans. Power Del.*, vol. 24, no. 1, pp. 20–29, Jan. 2009.

[15] A. Cavallini, G. Montanari, M. Tozzi, and X. Chen, "Diagnostic of HVDC systems using partial discharges," *IEEE Trans. Dielectr. Electr. Insul.*, vol. 18, no. 1, pp. 275–284, Feb. 2011.

[16] P. Moore, I. Portugues, and I. Glover, "A nonintrusive partial discharge measurement system based on RF technology," in *Proc. IEEE Power Eng. Soc. Gen. Meet.*, Jul. 2003, vol. 2, pp. 1–6.

[17] G. Robles, J. Martínez-Tarifa, M. Rojas-Moreno, R. Albarracín, and J. Ardila-Rey, "Antenna selection and frequency response study for UHF detection of partial discharges," in *Proc. IEEE I2MTC*, May 2012, pp. 1496–1499.

[18] Y. Shibuya, S. Matsumoto, M. Tanaka, H. Muto, and Y. Kaneda, "Electromagnetic waves from partial discharges and their detection using patch antenna," *IEEE Trans. Dielectr. Electr. Insul.*, vol. 17, no. 3, pp. 862–871, Jun. 2010.

[19] Y. Shibuya, S. Matsumoto, T. Konno, and K. Umezu, "Electromagnetic waves from partial discharges in windings and their detection by patch antenna," *IEEE Trans. Dielectr. Electr. Insul.*, vol. 18, no. 6, pp. 2013–2023, Dec. 2011.

[20] C. Balanis, *Antenna Theory: Analysis and Design*. New York: Wiley, 2005.

[21] Schwarzbeck Mess-Elektronik, UHALP 9108 A Data Sheet, Schönau, Germany. [Online]. Available: http://www.schwarzbeck.de

Guillermo Robles (SM'12) was born in Madrid, Spain, in 1969. He received the M.Sc. and Ph.D. degrees in electronic engineering from the Universidad Pontificia de Comillas de Madrid, Madrid, Spain, in 1993 and 2002, respectively.

In 2002, he joined the Departamento de Ingeniería Eléctrica, Universidad Carlos III de Madrid, Madrid, where he has been an Associate Professor since 2009 and is also with the High-Voltage Research and Tests Laboratory (LINEALT). He has coauthored more than 50 papers in international journals and conferences. His research interests include the design of sensors, instrumentation and measurement techniques for high frequency currents, particularly due to partial discharges in noisy environments, and the study and characterization of magneto-optic sensors based on the Faraday effect for the measurement of currents and the characterization of the behavior of magnetic materials at high frequencies.

Matilde Sánchez-Fernández received the M.Sc. degree in telecommunications engineering and the Ph.D. degree from Polytechnic University of Madrid, Madrid, Spain, in 1996 and 2001, respectively.

In 2000, she joined the Universidad Carlos III de Madrid, Madrid, where she has been an Associate Professor since 2009 teaching several undergraduate and graduate courses (M.Sc. and Ph.D.) related to communication theory and digital communications. Previously, she was a Telecommunication Engineer with Telefónica. She performed several research stays at the Information and Telecommunication Technology Center, The University of Kansas, Lawrence (1998), Bell Laboratories, Crawford Hill, NJ (2003–2006), Centre Tecnològic de Telecomunicacions de Catalunya, Barcelona, Spain (2007), and Princeton University, Princeton, NJ (2011). Her current research interests are multiple-input–multiple-output techniques, wireless communications, and simulation and modeling of communication systems, and in these fields, she has (co)authored more than 40 contributions to international journals and conferences.

Ricardo Albarracín Sánchez was born in Madrid, Spain, in 1983. He received the B.Sc. degree in technical electrical engineering and the M.Sc. degree in industrial electrical engineering from the Universidad Carlos III de Madrid (UC3M), Madrid, in 2005 and 2010, respectively, where he is currently working toward the Ph.D. degree in electrical engineering.

Since 2008, he has been an Assistant Professor with the Departamento de Ingeniería Eléctrica, UC3M. His subject was power grids with distributed generation and integration of renewable sources in power systems, mainly photovoltaic energy sources. In 2011, he joined the High-Voltage Research and Tests Laboratory (LINEALT), UC3M, where he is working on insulation systems diagnosis within power cables and electrical machines.

Mónica V. Rojas-Moreno was born in Duitama, Colombia, in 1979. She received the B.Sc. degree in electrical engineering from Universidad Industrial de Santander (UIS), Bucaramanga, Colombia, in 2003 and the M.Sc. and Ph.D. degrees in electrical engineering from the Universidad Carlos III de Madrid (UC3M), Madrid, Spain, in 2009 and 2011, respectively.

From 2003 to 2007, she was an Assistant Professor with the Escuela de Ingenierías Eléctrica, Electrónica y Telecomunicaciones, UIS. She is currently with the Departamento de Ingeniería Eléctrica and the High-Voltage Research and Tests Laboratory (LINEALT), UC3M. Her research interests include electromagnetic fields, partial discharges, instrumentation, high-frequency signals, and modeling of circuits.

Eva Rajo-Iglesias (SM'08) was born in Monforte de Lemos, Spain, in 1972. She received the M.Sc. degree in telecommunication engineering from the University of Vigo, Vigo, Spain, in 1996 and the Ph.D. degree in telecommunication from the Universidad Carlos III de Madrid (UC3M), Madrid, Spain, in 2002.

From 1997 to 2001, she was a Teacher Assistant with UC3M. In 2001, she joined the Polytechnic University of Cartagena, Cartagena, Spain, as Teacher Assistant for a year. She came back to UC3M as a Visiting Lecturer in 2002, and since 2004, she has been an Associate Professor with the Departamento de Teoría de la Señal y Comunicaciones, UC3M. Since 2009, she has been an Affiliate Professor with the Antenna Group, Signals and Systems Department, Chalmers University of Technology, Gothenburg, Sweden, where she was a Guest Researcher during autumn 2004, 2005, 2006, 2007, and 2008. Her main research interests include microstrip patch antennas and arrays, metamaterials and periodic structures, and optimization methods applied to electromagnetism. She has (co)authored more than 40 contributions in international journals and more than 80 in international conferences.

Dr. Rajo-Iglesias was a recipient of the 2007 Loughborough Antennas and Propagation Conference Best Paper Award and the "Best Poster Award in the field of Metamaterial Applications in Antennas" sponsored by The Institution of Engineering and Technology Antennas and Propagation Network, at Metamaterials 2009: Third International Congress on Advanced Electromagnetic Materials in Microwaves and Optics. She currently serves as Associate Editor for the IEEE ANTENNAS AND PROPAGATION MAGAZINE and for IEEE ANTENNAS AND WIRELESS PROPAGATION LETTERS.

Juan Manuel Martínez-Tarifa was born in Lorca, Spain, in 1975. He received the M.Sc. degree in electronic engineering and the M.Sc. degree in physics from the Universidad de Granada, Granada, Spain, in 1999 and 2000, respectively, and the Ph.D. degree in electrical engineering from the Universidad Carlos III de Madrid (UC3M), Madrid, Spain, in 2005.

He is currently an Associate Professor with the Departamento de Ingeniería Eléctrica, UC3M, where he was an Assistant Professor from 2000 to 2012. He has been a Visiting Researcher with Laboratoire de Génie Électrique, Université Paul Sabatier–Centre National de la Recherche Scientifique, Toulouse, France, and with Laboratorio di Ingegneria dei Materiali ed Alte Tensioni, Università di Bologna, Bologna, Italy. He is also currently a Technical Supervisor with the High-Voltage Research and Tests Laboratory (LINEALT), UC3M, where he is working on insulation systems diagnosis within power cables and electrical machines. He has published more than 20 articles in international journals and conferences. He has joined several research teams to work in more than ten research projects financed by public and private funds.